Oscillatory behavior of the domain wall dynamics in a curved cylindrical magnetic nanowire

R. Moreno,[1,2] V. L. Carvalho-Santos,[3,4] A. P. Espejo,[5] D. Laroze,[6,7] O. Chubykalo-Fesenko,[1] and D. Altbir[5,*]

[1]*Instituto de Ciencia de Materiales de Madrid, CSIC, Cantoblanco, 28049 Madrid, Spain*

[2]*Department of Physics, University of York, Heslington, York YO10 5DD, United Kingdom*

[3]*Instituto Federal de Educação, Ciência e Tecnologia Baiano, 48970-000 Senhor do Bonfim, Brazil*

[4]*Departamento de Física, Universidade Federal de Viçosa, Avenida Peter Henry Rolfs s/n, 36570-000 Viçosa, MG, Brazil*

[5]*Departamento de Física, CEDENNA, Universidad de Santiago de Chile, Avenida Ecuador 3493, Santiago, Chile*

[6]*Instituto de Alta Investigación, CEDENNA, Universidad de Tarapacá, Casilla 7D, Arica, Chile*

[7]*School of Physical Sciences and Nanotechnology, Yachay Tech University, 00119 Urcuquí, Ecuador*

(Received 30 May 2017; published 1 November 2017)

Understanding the domain wall dynamics is an important issue in modern magnetism. Here we present results of domain wall displacement in curved cylindrical nanowires at a constant magnetic field. We show that the average velocity of a transverse domain wall increases with curvature. Contrary to what is observed in stripes, in a curved wire the transverse domain wall oscillates along and rotates around the nanowire with the same frequency. These results open the possibility of new oscillation-based applications.

DOI: 10.1103/PhysRevB.96.184401

I. INTRODUCTION

The understanding of the domain wall (DW) dynamics is a cornerstone in nanomagnetism owing to the potential technological applications in modern nanoelectronics such as high density memories [1] and logic devices [2]. In particular, the promising concept of "race-track memory" [1,3] demands a well-controlled motion of the DW along a nanowire. In this context, several works have studied the controlled displacement of DWs in stripes [4–9] and cylindrical wires [10–12]. Such studies have revealed that geometry plays a fundamental role in the DW dynamics. For instance, rectangular wires exhibit a Walker field [13]; that is, while at low fields the DW velocity is linearly proportional to the field, at some critical value the velocity drastically drops and an oscillatory behavior of the DW position is observed [8]. On the contrary, in cylindrical nanowires, the DW does not change its structure during the motion and thus no Walker limit or critical velocity is observed [11]. Other examples of important geometrical effects on the DW motion are an increase of the DW velocity by a factor of 4 if a magnetic stripe has a series of cross-shaped traps [14] or the pinning of the DW by artificial necks in wires [15].

Since the shape of the nanowire, frequently curved by nature, affects the magnetization statics and dynamics [16], and many of the potential applications of the DW include curvilinear segments along the wire (see, for example, Ref. [1]), it is fundamental to understand how the curvature influences the DW dynamics. Recent theoretical studies have shown that new interesting phenomena appear when a cylindrical wire is curved. First, it has been shown that due to a curvature-induced Dzyaloshinsky-Moriya interaction (DMI), the DW gets pinned at the maximum of the curvature and, to minimize the exchange cost, a phase selectivity occurs; that is, a head-to-head DW is directed outward while a tail-to-tail DW is directed inward the bend [17]. This curvature-induced DMI is also responsible for the formation of a new DW profile, given by a head-to-head vortex-antivortex pair in toroidal magnetic nanoparticles [18]. Recently, the effects of the curvature on a magnetic helicoid ribbon as well as on a Möbius ribbon have been analyzed [19]. It has also been shown that the spin-current driven DW motion is strongly dependent on curvature and torsion [20]. In this case, the curvature results in the existence of a Walker limit for a uniaxial wire, and the torsion induces an effective shift of the nonadiabatic spin torque parameter [20]. The direction of motion of a DW along a helical wire under the action of a Rashba spin-orbit torque depends on the helix chirality and wall charge in such a way that DWs can be moved only under the action of Rashba and geometrical effects [21]. Thus, the curvature can induce inhomogeneities in the DW profile. Under this frame, the study of the influence of curvature on the DW velocity is paramount.

In this paper, by means of an analytical model and micromagnetic simulations, we explore the dynamics of a transverse DW in a curved cylindrical nanowire driven by a constant external magnetic field. We have analyzed the DW motion for different curvatures of the nanowire, going from 0 until it reaches its maximum, which is a half-torus section. Our results demonstrate a strong dependence of the DW dynamics on the curvature of the wire, leading to the possibility of engineering its characteristic features. The manuscript is organized as follows. In Sec. II, the analytical model for a curved nanowire is developed and an effective equation of motion for the DW is presented. In Sec. III, numerical simulations using NMAG micromagnetic software [22] are performed for different control parameters. Finally, conclusions are presented in Sec. IV.

II. THEORETICAL MODEL

Let us consider a curved wire with length L and diameter d characterized by a magnetization, $\mathbf{M}$. Its dynamics is modeled by the Landau-Lifshitz-Gilbert (LLG) equation

$$\frac{\partial \mathbf{m}}{\partial \tau} = \mathbf{m} \times \frac{\delta \mathcal{E}}{\delta \mathbf{m}} + \alpha\, \mathbf{m} \times \frac{\partial \mathbf{m}}{\partial \tau}, \tag{1}$$

where $\mathbf{m} = \mathbf{M}/M_S$, such that M_S is the saturation magnetization. Here, we use dimensionless time $\tau = t\gamma_0 M_s$ and dimensionless energy $\mathcal{E} = E/(\mu_0 M_S^2 V)$, such that V is the

*dora.altbir@usach.cl

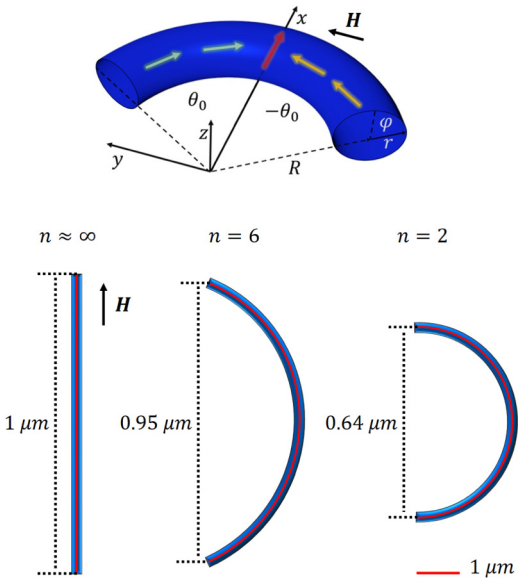

FIG. 1. The top figure shows the adopted coordinate system to describe the curved wire, the magnetization direction, and the domain wall. The bottom figures show different nanowires with their corresponding n values and dimensions. All the wires have 1 μm of length along their axis, which is indicated with red lines.

volume, μ_0 is the magnetic permeability, and $\gamma_0 = \mu_0|\gamma|$, with $\gamma = 1.76 \times 10^{11} rad/Ts$ being the gyronagnetic factor. Additionally, α is the dimensionless Gilbert damping parameter. In our calculations, we consider a Permalloy wire characterized by the saturation magnetization $\mu_0 M_s = 1T$ and the exchange constant $A = 1.3 \times 10^{-11} J/m$ and we fix the damping constant to $\alpha = 0.01$.

The geometrical description of a curved nanowire is done by using a toroidal coordinate system, given by

$$\mathbf{r} = \hat{e}_R\,(r + R\cos\theta) + \hat{\theta}\,R\sin\theta\,, \tag{2}$$

where $\hat{e}_R$ and $\hat{\theta}$ are the radial unitary vector and the angular unitary vector, respectively, with R and r as the toroidal and poloidal radii, respectively. The angles $\theta \in [-\theta_0,\theta_0]$ and $\varphi \in [0,2\pi]$ play the role of azimuthal and poloidal angles, respectively, as is shown in Fig. 1. This parametrization allows us to define the wire length as $L = 2\theta_0 R$, which is fixed in this work. Even though this parametrization yields a geometry with variable Gaussian curvature, in this work we define the curvature of the wire as $K = 1/R$. Then, variations in the curvature are represented by simultaneous changes in the toroidal radius $R = nL/2\pi$ and the azimuthal angle $\theta \in [-\pi/n : \pi/n]$, where $n \in [2,\infty)$ is a real number (see Fig. 1). It can be noted that the wire with greater curvature, described by a half-torus section, is obtained when $\theta_0 = \pi/2$, and an almost straight wire is obtained for $n \to \infty$. The description of such a curved wire by its toroidal and poloidal radii is more suitable than other representations [23–25].

Let us parametrize the magnetization $\mathbf{m}$ in the spherical coordinate system lying on a curvilinear background described by a Frenet-Serret basis $(\hat{\theta}, -\hat{e}_R, \hat{z})$, that is, $\mathbf{m} = \hat{\theta}\cos\Theta - \hat{e}_R\sin\Theta\cos\Phi + \hat{z}\sin\Theta\sin\Phi$, where the directional vectors are associated with a toroidal coordinate system given in Eq. (2).

The LLG equations in this coordinate system can be written as

$$-\sin\Theta\frac{\partial\Theta}{\partial\tau} = \frac{\delta\mathcal{E}}{\delta\Phi} + \alpha\,\sin^2\Theta\,\frac{\partial\Phi}{\partial\tau} \tag{3}$$

and

$$\sin\Theta\frac{\partial\Phi}{\partial\tau} = \frac{\delta\mathcal{E}}{\delta\Theta} + \alpha\,\frac{\partial\Theta}{\partial\tau}. \tag{4}$$

For the energy, we employ a simple model that contains only tree contributions: exchange, magnetostatic, and Zeeman. Hence, the energy can be written as

$$E = S\,R\int_{-\theta_0}^{\theta_0}\left[\ell^2 E_{\rm ex} - \lambda\cos^2\Theta - \frac{\ell^2}{A}\mathbf{H}\cdot\mathbf{M}\right]d\theta\,, \tag{5}$$

where $S = \pi r^2$ is the area of the wire cross section, $\ell = \sqrt{A/(\mu_0 M_S^2)}$, $E_{\rm ex}$ is the exchange energy density, $\mathbf{H} = H(\hat{\theta}\cos\theta - \hat{e}_R\sin\theta)$ is the external magnetic field pointing along the y-axis direction, and λ is the dimensionless anisotropy constant. Following the model described in Refs. [17,20], we consider that $\lambda > 0$ represents an easy-tangential anisotropy coming from magnetostatic contributions. It is worth noting that there is a dependence of λ on θ and φ, coming from the fact that the demagnetizing field depends on the geometry of the magnetic body [26]. However, because of the considered dimensions, this difference is small, and we adopt $\lambda = 1/4$ to describe magnetostatic contributions to the energy [8,17,20]. In terms of the adopted parametrization, the exchange energy density is given by [17,27]

$$\frac{E_{\rm ex}}{K^2} = \left(\frac{\partial\Theta}{\partial\theta} + \cos\Phi\right)^2 + \left(\sin\Theta\frac{\partial\Phi}{\partial\theta} - \cos\Theta\sin\Phi\right)^2. \tag{6}$$

The DW properties can be analyzed based on a collective variable approach [28,29]. In this manner, a *head-to-head* DW can be described by the ansatz

$$\Theta(\theta,\tau) = 2\arctan\left[\exp\left(\frac{\zeta(\theta,\tau)}{\Delta}\right)\right], \quad \Phi(\tau) = \phi(\tau), \tag{7}$$

where $\zeta(\theta,\tau) = R\theta - q(\tau)$. Here q and ϕ denote the canonically conjugated pairs of collective variables, determining the DW position and phase, respectively, and Δ determines the DW width, which is assumed to be constant and independent on the DW position or the direction. This approximation is valid once the considered geometry does not present torsion and a generalized DW model [30] is not necessary. From Eqs. (6) and (7), it can be noted that in the absence of an external magnetic field, the minimum energy density is obtained for $\Phi_0 = \pi$ and the DW has its minimum energy when it points along $\hat{e}_R$ (outward the bend), according to Yershov *et al.* [17].

The energy of the DW can be obtained analytically by performing the substitution of Eq. (7) in Eq. (5) but its expression is cumbersome and therefore is presented in the Appendix. The dynamical properties of the domain wall in terms of the collective variables can be described by the

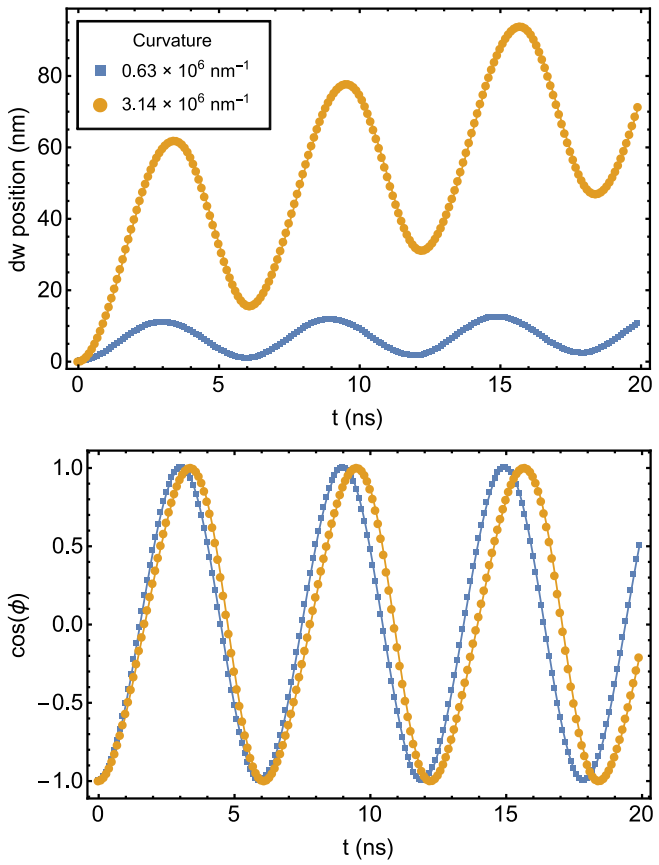

FIG. 2. Domain wall position, q (top), and phase, ϕ (bottom), obtained from the numerical integration of Eqs. (8) and (9). The used value of the magnetic field is $H = 6$ mT.

following equations of motion [17]:

$$\dot{q} = \frac{1}{2S}\frac{\partial \mathcal{E}_{DW}}{\partial \phi} + \alpha\,\Delta\,\dot{\phi} \tag{8}$$

and

$$\dot{\phi} = -\frac{1}{2S}\frac{\partial \mathcal{E}_{DW}}{\partial q} - \frac{\alpha}{\Delta}\,\dot{q}\,, \tag{9}$$

which have been derived by inserting the ansatz (7) into Eqs. (3) and (4), respectively. The above equations do not have simple analytical solutions; nevertheless, they can be solved numerically. The obtained DW position and phase are shown in Fig. 2 for a fixed value of the magnetic field $H = 6$ mT. The upper frame shows the oscillatory behavior of the DW center along the wire. The lower frame presents the DW phase for the angular velocity of the DW rotation around the wire. The period of the DW displacement is approximately 6 ns, and in this time interval the phase changes in 2π, giving a precessional frequency of 60° per nanosecond. This behavior of the DW direction is different from that of stripes, which present a 180° rotation around the nanowire followed by an inversion of the sense of the rotation. This difference can be explained because nanostripes have two minima associated with the magnetostatic energy when the DW is pointing along the thinner sides of the stripe (exchange energy is equal during all the DW motion). On the other hand, the DW magnetic energy presents only one minimum in a curved cylindrical wire, which is mainly associated with the exchange energy. However, in curved cylindrical wires the DW has different values of the exchange energy when it is pointing inward or outward of the bent of the wire. Then, the DW needs to rotate an angle 2π before recovering its minimum energy position. Let us also remark that unlike its straight counterpart, curved wires present the oscillatory behavior associated with the Walker breakdown phenomenon. As explained in Ref. [11], the Walker breakdown is absent in straight cylindrical wires because the demagnetizing factors and the exchange effective field do not depend on the DW phase. Therefore the contribution coming from the magnetostatic and exchange energies to the effective fields acting on the domain wall (which produces the Walker breakdown) is canceled upon derivatives and do not contribute to the DW displacement. In the case of a curved wire, the corresponding effective fields depend on the DW phase (see the Appendix), and therefore, there will be always an oscillatory behavior in the DW position during its displacement.

We remark that our model provides quantitative results which are valid not far from the nanowire center. Since the magnetic field is applied along the y-axis direction, the torque produced by the field is maximum when the domain wall is at the center of the magnetic wire. When we are far from the center, the domain wall experiences a smaller torque and, although the qualitative behavior is exactly the same, the velocity slows down.

III. NUMERICAL RESULTS

To better understand our analytical results, we developed several full numerical simulations. We use the public micromagnetic code NMAG [22], which considers finite element discretization, allowing a better description of curved surfaces compared to finite differences methods. With this code we solve the Landau-Lifshitz-Gilbert equation (1) for a Py nanowire. Since we focus on a *head-to-head* DW, the position of the center of the DW is obtained from $m_{\|}(\mathbf{r}_{DW},t) = 0$, where $m_{\|}$ is the parallel component along the wire axis. Using the angular difference $\triangle\theta$ between the position of the center of the DWs at two consecutive times, we define the instantaneous velocity as $\mathrm{V}(t) = R\,\triangle\,\theta/\,\triangle\,t$. All the simulated wires have the same diameter ($d = 30$ nm) and length ($L = 1\ \mu$m), but different curvatures (K), which were varied as a function of n. The initial state of all simulations is a transverse DW in a wire, obtained by saturating the system in the $+x$ direction with a $1T$ field. Then, the field is switched off, and the system is left to relax to its equilibrium state, as explained in Ref. [31]. In this way we create a head-to-head DW pointing along the $+x$ direction (outward the bend), as predicted in Ref. [17]. Starting from this state, we apply a constant magnetic field along the $+y$ direction and perform the simulation for 20 ns. To check our methodology we have obtained the velocity from our simulations in straight wires and compared our results with the velocity obtained in the literature [11] for similar systems. Both results are in good agreement, giving us confidence in the software and method used in our calculations.

Figure 3 illustrates snapshots at different times of the reversal process of the DW propagation along a wire with curvature $K \approx 3.14 \times 10^6\ \mathrm{nm}^{-1}$. In these snapshots a rotation of the DW around the wire axis as well as an oscillation along

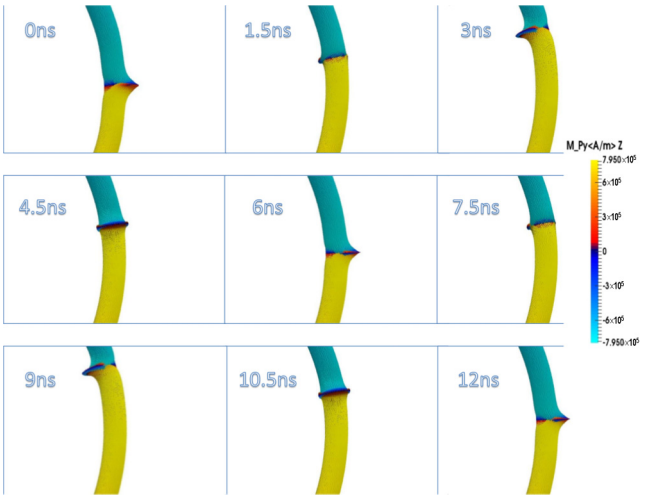

FIG. 3. Schematic representation of the oscillatory movement of the DW pushed by a constant magnetic field. The wire has a maximum curvature of $1/R \approx 3.14 \times 10^6$ nm^{-1}.

its axis is shown. It should be highlighted that the sense of the rotation of the DW is constant. The DW oscillations along the propagation line have been observed in previous works for DW dynamics in nanostripes under the action of a constant magnetic field [8,9,32]. However, in the case of a Py stripe, the DW displacement oscillates with a frequency double the rotation frequency of the wall around the stripe [8,9]. In the present study, as is clearly seen in Fig. 3, and in agreement with our theoretical predictions, we have observed that the period of the DW displacement along the wire is exactly the same as the rotation period around it.

The dynamics of the DW position is shown in Fig. 4. We observe that it has an oscillatory behavior and its amplitude depends on the curvature, also in agreement with the analytical model. In fact, both approaches exhibit the same oscillation period. The discrepancy in the exact DW position obtained from both methods comes from the fact that the theoretical model fixes the width of the DW, however simulations show a small change in the width during rotation.

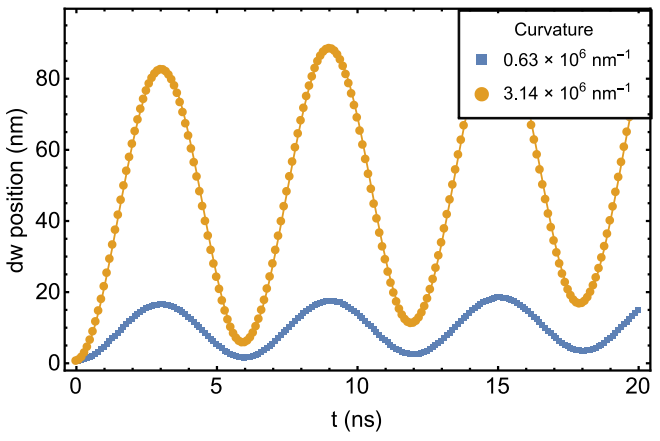

FIG. 4. Displacement of the domain wall center as a function of time for two different curvatures at $H = 6$ mT found using NMAG simulations.

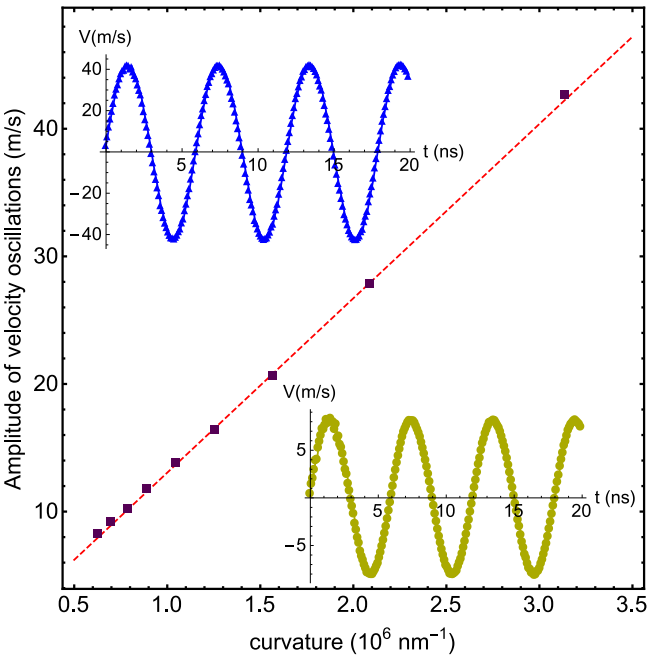

FIG. 5. Amplitude of velocity oscillation as a function of the curvature at $H = 6$ mT. Insets show the velocity of the DW for wires with curvatures of 3.14×10^6 nm^{-1} (blue triangles) and 0.63×10^6 nm^{-1} (beige dots).

Despite the existence of an oscillatory behavior of the DW position, an increase in the curvature implies an increment in the average amplitude of the velocity oscillation. This occurs because, as shown in Fig. 1, the change in the direction of a magnetic moment when passing the DW is smaller in a curved wire, as compared to what occurs in a straight structure. Based on our results, we have obtained the amplitude of the DW velocity as a function of the wire curvature. Our simulations show that the amplitude of the velocity oscillation does not depend on the applied magnetic field, varying only with the shape of the nanowire. In fact, the amplitude of the velocity is a linear function of the curvature, as shown in Fig. 5.

Finally, Fig. 6 shows the average of the DW velocity as a function of the external field for different curvature values.

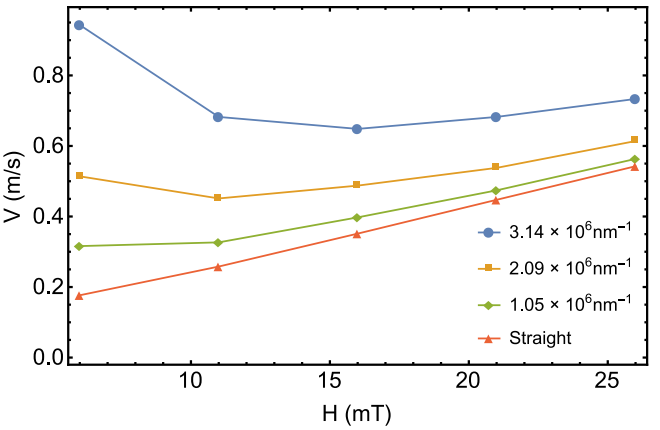

FIG. 6. Average velocity as a function of the external magnetic field for different curvatures.

We can observe that the average velocity is no longer a linear function of the magnetic field when the wire is curved. Increasing the curvature produces a more noticeable change of the linear behavior. Our modeling shows that at very small fields of the order of 1 mT (not shown due to their too small values) the linear regime is recovered in these nanowires. In this sense, the Walker breakdown, absent in straight cylindrical wires [11], is observed in nanowires with large curvature.

IV. CONCLUSIONS

In this paper we studied domain wall propagation in curved cylindrical nanowires showing an oscillatory behavior along and around the nanowire axis. Contrary to the case of rectangular stripes, the rotational period was proven to be the same as the oscillations in the DW position. The amplitude of the velocity depends on the magnitude of the demagnetizing field that, in turn, depends on the curvature. The frequency of these oscillations is a linear function of the external magnetic field. The average velocity is not linear in the applied field and, contrary to what happens in stripes, curved nanowires show the Walker breakdown phenomenon. The oscillation of the domain wall around and along the nanowire provides a unique opportunity to convert a constant magnetic field to a radio-frequency signal with tunable parameters coming from nanowire geometry, material, and curvature. Such oscillations should be also possible in the presence of spin currents, which could open novel possibilities for spin-torque oscillators based on magnetic nanowires.

ACKNOWLEDGMENTS

In Chile, we thank the following for partial financial support: the Centers of Excellence with BASAL/CONICYT financing (Grant No. FB0807), Fondecyt (Grant No. 1160198), and CONICYT-ANILLO-ATC 1410. In Brazil, we thank the CNPq (Grants No. 301015/2015-5 and No. 401132/2016-1) and Fapesb (Grant No. JCB0063/2016). We thank the Spanish Ministry of Economy and Competitiveness (Grants No. MAT2013-47078-C2-2-P, No. MAT2016-76824-C3-1-R, and No. FIS2016-78591-C3-3-R). We are also grateful to V. P. Kravchuk for fruitful discussions on the theoretical model.

APPENDIX: DOMAIN WALL ENERGY

We have considered that the magnetic energy of the wire under an external magnetic field has three contributions: $E = E_{\rm ex} + E_{\rm dip} + E_Z$, where $E_{\rm ex}$ is the exchange energy, $E_{\rm dip}$ is an effective dipolar energy represented by an in-surface anisotropy, and E_Z is the Zeeman energy. The general expressions of the energy are given by Eqs. (5) and (6). Inserting the DW's ansatz (7) into the aforementioned equations we obtain

$$E_{\rm ex} = \frac{\ell^2 S}{R^2}\left[L + 4R\,\Lambda(q)\,\cos\phi + \frac{2R^2 - \Delta^2 + \Delta^2\cos 2\phi}{\Delta}\,\Omega(q)\right], \tag{A1}$$

where

$$\Lambda(q) = \arctan\left[\exp\left(\frac{-q + L/2}{\Delta}\right)\right] - \operatorname{arccot}\left[\exp\left(\frac{q + L/2}{\Delta}\right)\right]$$

and

$$\Omega(q) = \frac{\sinh\left(\frac{L}{\Delta}\right)}{\left[\cosh\left(\frac{2q}{\Delta}\right) + \cosh\left(\frac{L}{\Delta}\right)\right]},$$

The dipolar energy is given by an in-surface anisotropy, being evaluated as

$$E_{\rm dip} = 2S\lambda\left[\Delta\,\Omega(q) - \frac{L}{2}\right]. \tag{A2}$$

Finally, the energy from the interaction with the external magnetic field is given by

$$\begin{aligned} E_Z = \frac{ie^{-i\theta_0}HSR}{2}\Bigg\{ & 2 - 2e^{2i\theta_0} + (\cos\phi - 1)\left[{}_2F_1\left(1,-\frac{i\Delta}{R},1-\frac{i\Delta}{R},-ie^{\frac{-q+L/2}{\Delta}}\right) + {}_2F_1\left(1,\frac{i\Delta}{R},1+\frac{i\Delta}{R},ie^{\frac{-q-L/2}{\Delta}}\right)\right] \\ & - e^{2i\theta_0}(\cos\phi - 1)\left[{}_2F_1\left(1,-\frac{i\Delta}{R},1-\frac{i\Delta}{R},-ie^{\frac{-q-L/2}{\Delta}}\right) + {}_2F_1\left(1,\frac{i\Delta}{R},1+\frac{i\Delta}{R},ie^{\frac{-q+L/2}{\Delta}}\right)\right] \\ & - (\cos\phi + 1)\left[{}_2F_1\left(1,-\frac{i\Delta}{R},1-\frac{i\Delta}{R},ie^{\frac{-q+L/2}{\Delta}}\right) + {}_2F_1\left(1,\frac{i\Delta}{R},1+\frac{i\Delta}{R},-ie^{\frac{-q-L/2}{\Delta}}\right)\right] \\ & + e^{2i\theta_0}(\cos\phi + 1)\left[{}_2F_1\left(1,-\frac{i\Delta}{R},1-\frac{i\Delta}{R},ie^{\frac{-q-L/2}{\Delta}}\right) + {}_2F_1\left(1,\frac{i\Delta}{R},1+\frac{i\Delta}{R},-ie^{\frac{-q+L/2}{\Delta}}\right)\right]\Bigg\}, \end{aligned} \tag{A3}$$

where ${}_2F_1(a,b,c,z)$ is the hypergeometric function.

Aiming to understand the difference between the DW dynamics in curved and straight wires, we study an approximation in which the DW is near to the center of the wire and its width is much smaller than the wire length. In this case q is on the order

of tens nanometers, and therefore $\Delta/L \sim 10^{-3}$. Consequently, Eqs. (A1) and (A2) are simplified to

$$E_{\mathrm{ex}_{\Delta/L\to 0}} \approx \frac{\ell^2 S}{R^2}\left[L + \frac{2R^2}{\Delta} + 2\pi\ R\cos\phi\right], \tag{A4}$$

$$E_{\mathrm{dip}_{\Delta/L\to 0}} \approx -\lambda\, V, \tag{A5}$$

where V is the wire volume. By use of the considered limits, the functions $\Lambda(q)$ and $\Omega(q)$ are reduced to $\Lambda(q) \approx \pi/2$ and $\Omega(q) \approx 1$. Even with these approximations, the Zeeman energy keeps its dependence on q and ϕ, which results in the oscillatory behavior of DW dynamics in curved nanowires. On the other hand, a straight wire is obtained in the limit $R \to \infty$ and then $E_{\mathrm{ex}_{R\to\infty}} \approx 2\ell^2 S/\Delta$, while dipolar energy keeps the form presented in Eq. (A5). In addition, by taking the derivatives of the Zeeman energy and adopting the limit $R \to \infty$, it can be shown that $\partial E_{Z_{R\to\infty}}/\partial q = -2HS$ and $\partial E_{Z_{R\to\infty}}/\partial\phi = 0$. Therefore, by substituting these results in Eqs. (8) and (9) and performing some algebraic manipulation, we obtain that the DW velocity in a straight wire is

$$\dot{q} = \frac{\alpha\Delta}{1+\alpha^2} H, \tag{A6}$$

which is the equation of motion for DW along a straight wire [8,9].

[1] S. S. P. Parkin, M. Hayashi, and L. Thomas, Science **320**, 190 (2008).

[2] D. A. Allwood, G. Xiong, M. D. Cooke, C. C. Faulkner, D. A. N. Vernier, and R. P. Cowburn, Science **296**, 2003 (2002).

[3] G. Catalan, J. Seidel, R. Ramesh, and J. F. Scott, Rev. Mod. Phys. **84**, 119 (2012).

[4] G. S. D. Beach, C. Nistor, C. Knutson, M. Tsoi, and J. L. Erskine, Nat. Mater. **4**, 741 (2005).

[5] I. M. Miron, T. Moore, H. Szambolics, L. D. Buda-Prejbeanu, S. Auffret, B. Rodmacq, S. Pizzini, J. Vogel, M. Bonfim, A. Schuhl, and G. Gaudin, Nat. Mater. **10**, 419 (2011).

[6] S. Emori, U. Bauer, S.-M. Ahn, E. Martinez, and G. S. D. Beach, Nat. Mater. **12**, 611 (2013).

[7] J.-S. Kim, M.-A. Mawass, A. Bisig, B. Krüger, R. M. Reeve, T. Schulz, F. Büttner, J. Yoon, C.-Y. You, M. Weigand, H. Stoll, G. Schütz, H. J. M. Swagten, B. Koopmans, S. Eisebitt, and M. Kläui, Nat. Commun. **5**, 3429 (2014).

[8] D. G. Porter and M. J. Donahue, J. Appl. Phys. **95**, 6729 (2004).

[9] A. Mougin, M. Cormier, J. P. Adam, P. J. Metaxas, and J. Ferré, Europhys. Lett. **78**, 57007 (2007).

[10] R. Hertel, J. Magn. Magn. Mater. **249**, 251 (2002).

[11] M. Yan, A. Kákay, S. Gliga, and R. Hertel, Phys. Rev. Lett. **104**, 057201 (2010).

[12] R. Wieser, E. Y. Vedmedenko, P. Weinberger, and R. Wiesendanger, Phys. Rev. B **82**, 144430 (2010).

[13] N. L. Schryer and L. R. Walker, J. Appl. Phys. **45**, 5406 (1974).

[14] E. R. Lewis, D. Petit, L. O'Brien, A. Fernandez-Pacheco, J. Sampaio, A.-V. Jausovec, H. T. Zeng, D. E. Read, and R. P. Cowburn, Nat. Mater. **9**, 980 (2010).

[15] A. Himeno, T. Ono, S. Nasu, K. Shigeto, K. Mibu, and T. Shinjo, J. Appl. Phys. **93**, 8430 (2003).

[16] Y. Gaididei, V. P. Kravchuk, and D. D. Sheka, Phys. Rev. Lett. **112**, 257203 (2014).

[17] K. V. Yershov, V. P. Kravchuk, D. D. Sheka, and Y. Gaididei, Phys. Rev. B **92**, 104412 (2015).

[18] S. Vojkovic, V. L. Carvalho-Santos, J. M. Fonseca, and A. S. Nunez, J. Appl. Phys. **121**, 113906 (2017).

[19] Y. Gaididei, A. Goussev, V. P. Kravchuk, O. V. Pylypovskyi, J. M. Robbins, D. D. Sheka, V. Slastikov, and S. Vasylkevych, J. Phys. A: Math. Theor. **50**, 385401 (2017).

[20] K. V. Yershov, V. P. Kravchuk, D. D. Sheka, and Y. Gaididei, Phys. Rev. B **93**, 094418 (2016).

[21] O. V. Pylypovskyi, D. D. Sheka, V. P. Kravchuk, K. V. Yershov, D. Makarov, and Y. Gaididei, Sci. Rep. **6**, 23316 (2016).

[22] T. Fischbacher, M. Franchin, G. Bordignon, and H. Fangohr, IEEE Trans. Magn. **43**, 2896 (2007).

[23] I. S. Gradshteyn and I. M. Ryzhik, *Table of Integral, Series and Products*, 7th ed. (Academic Press, New York, 2007).

[24] V. L. Carvalho-Santos, W. A. Moura-Melo, and A. R. Pereira, J. Appl. Phys. **108**, 094310 (2010).

[25] M. Bellegia, M. de Graef, and Y. T. Millev, Proc. R. Soc. London, Ser. A **465**, 3581 (2009).

[26] A. Aharoni, *Introduction to the Theory of Ferromagnetism* (Oxford University Press, New York, 1996).

[27] D. D. Sheka, V. P. Kravchuk, and Y. Gaididei, J. Phys. A **48**, 125202 (2015).

[28] J. C. Slonkzewski, Phys. Rev Lett. **29**, 1679 (1972).

[29] A. A. Thiele, Phys. Rev. Lett. **30**, 230 (1973).

[30] V. P. Kravchuk, J. Magn. Magn. Mater. **367**, 9 (2014).

[31] E. Saitoh, H. Miyajima, T. Yamaoka, and G. Tatara, Nature (London) **432**, 203 (2004).

[32] Y. S. Choi, J. Y. Lee, M. W. Yoo, K. S. Lee, K. Y. Guslienko, and S. K. Kim, Phys. Rev. B **80**, 012402 (2009).